Molecular Cell, Vol. 20, 633–643, November 23, 2005, Copyright ©2005 by Elsevier Inc. DOI 10.1016/j.molcel.2005.09.017

An Essential GTPase Promotes Assembly of Preribosomal RNA Processing Complexes

Katrin Karbstein,[1] Stefanie Jonas,[1] and Jennifer A. Doudna[1,2,3,*]
[1]Department of Molecular and Cell Biology
[2]Department of Chemistry
[3]Howard Hughes Medical Institute
University of California, Berkeley
Berkeley, California 94720

Summary

Ribosome biogenesis in eukaryotes is a highly regulated process involving hundreds of transiently associated proteins and RNAs. Although most of these assembly factors have been genetically linked to specific step(s) in the biogenesis pathway, their biochemical functions are generally unknown. Bms1, an essential protein in yeast, is the only known GTPase required for biosynthesis of the 40S ribosomal subunit and interacts with Rcl1, an essential protein suggested to be an endonuclease. Here, we show thermodynamic coupling in the binding of Bms1 to GTP, Rcl1, and U3 *s*mall *n*ucleo*l*ar RNA (snoRNA), an essential RNA that base pairs to pre-rRNA. Rcl1 binding to preribosomes is severely limited in yeast cells expressing a Bms1 mutant defective for Rcl1 binding. Additionally, we provide evidence that the C-terminal domain of Bms1 acts as an intramolecular GTPase-activating protein. Together, these data suggest that Bms1 functions as a GTP-regulated switch to deliver Rcl1 to preribosomes, providing molecular insight into preribosome assembly.

Introduction

Ribosome biogenesis in eukaryotes is a conserved, complex, and highly regulated process that in the yeast *Saccharomyces cerevisiae* involves dozens of small RNAs as well as >170 *trans*-acting protein factors (Fromont-Racine et al., 2003). These factors orchestrate modification and processing of the initial 35S precursor ribosomal RNA (rRNA) transcript into the mature 18S, 5.8S, and 25S rRNAs; folding of the rRNA; and binding of ribosomal proteins and 5S rRNA (Fromont-Racine et al., 2003; Venema and Tollervey, 1999). During or shortly after transcription, the rRNA is methylated and pseudouridylated at specific residues. Once transcription is completed, at least 11 endonucleolytic and exonucleolytic cleavage steps are required to generate the mature 5′ and 3′ ends of 18S, 5.8S, and 25S rRNA (Figure 1A). Although rRNA modification, directed by snoRNAs, is now fairly well understood (Decatur and Fournier, 2003; Kiss, 2002), pre-rRNA processing remains much less well defined. Although the order of processing reactions has been elucidated, only two of the seven endonucleolytic steps have enzymes assigned to them, with the remaining endonucleases currently unknown. For other steps, it is not yet clear whether processing occurs endonucleolytically or exonucleolytically (see legend to Figure 1A). How the processing factors are recruited to preribosomes remains to be elucidated, along with the questions of how rRNA folding and protein assembly onto the RNA are organized and how these processes are integrated.

Electron microscopy conducted in the late 1960s showed that large complexes assemble at the 5′ ends of nascent rRNA transcripts as they emanate from a central chromatin core (Miller and Beatty, 1969; Osheim et al., 2004) (Figure 1B). Components of these complexes in yeast, required for biogenesis of the 40S subunit, include at least 28 proteins and the snoRNA U3 (Dragon et al., 2002; Grandi et al., 2002; Kass et al., 1990). U3 snoRNA, an ~330 nt molecule that is complementary to short regions within the pre-rRNA (Figure 1B), binds to preribosomes to form a complex essential to ribosome biogenesis and cell viability (Beltrame et al., 1994; Beltrame and Tollervey, 1992, 1995). However, neither the role of U3 snoRNA nor its associated proteins is yet understood.

One intriguing component of the U3 snoRNA-containing complex is Bms1, a 136 kDa protein that is essential in yeast and is conserved throughout the eukaryotic kingdom. Its N-terminal domain is homologous to GTPases of the Ras superfamily, suggesting a possible regulatory function during biogenesis of the 40S ribosomal subunit (Figure 1C) (Gelperin et al., 2001; Sanchez and Sali, 1998; Wegierski et al., 2001). Two-hybrid data and copurification experiments indicated that Bms1 binds to Rcl1, another essential protein involved in ribosome biogenesis (Grandi et al., 2002; Krogan et al., 2004; Wegierski et al., 2001). Rcl1, a 40 kDa protein with sequence homology to RNA 3′ cyclases (Billy et al., 2000), does not appear to have cyclase activity and instead has been proposed to be one of the elusive pre-rRNA endonucleases (Billy et al., 2000). To understand the role of these key proteins in the production of mature 40S ribosomal subunits, we have taken a biochemical approach intended to complement the groundbreaking genetic and proteomic experiments used in the field to date. We have cloned and purified Bms1 and show that it is capable of robust GTP hydrolytic activity. Furthermore, our data establish a direct interaction between Bms1 and Rcl1. Interestingly, Bms1 also binds to U3 snoRNA. A quantitative analysis of the interdependence of these biochemical activities suggests a model in which Bms1 binds Rcl1 in a GTP-dependent manner and, via its affinity to U3 snoRNA, delivers it to preribosomes. This model implies that Bms1 can control access of preribosomal RNA intermediates to Rcl1 during ribosome biogenesis, enabling temporal function of Rcl1 as a structural component or catalyst during ribosome assembly.

Results

To study its role in ribosome biogenesis, Bms1 protein was purified from *E. coli*. Although the full-length Bms1 (136 kDa, 1183 amino acids) was poorly expressed and

*Correspondence: doudna@berkeley.edu

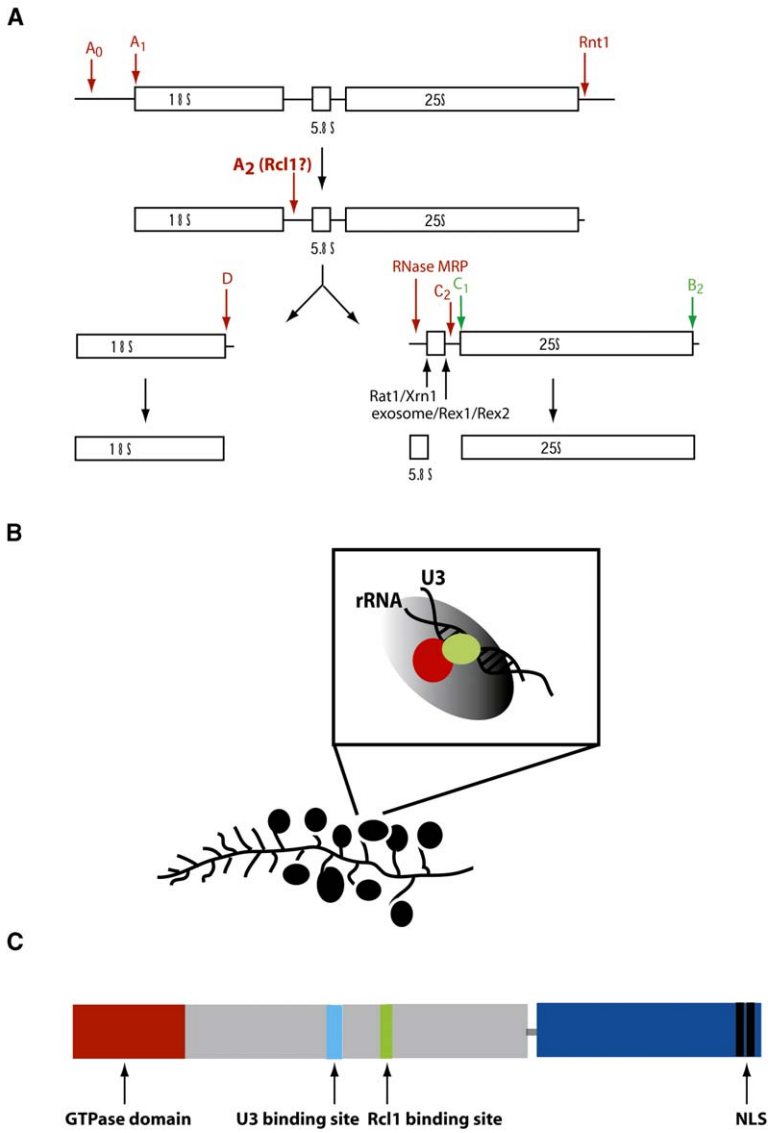

Figure 1. Bms1 and Rcl1 Form a Subcomplex within Preribosomes

(A) Schematic of the pre-rRNA processing pathway (adapted from: Venema and Tollervey, 1999). Cleavage steps by endonucleases are shown in red, processing steps by exonucleases are shown in black, and steps where it is unknown whether they are executed by endo- or exonucleases are shown in green. Pre-rRNA processing is initiated by Rnt1 cleavage at the 3′ end of the transcript. This is followed by cleavage at sites A_0 and A_1 by unknown endonucleases. Cleavage at site A_2 has been suggested to be performed by Rcl1 (Billy et al., 2000) and results in separation of the RNAs for the small and large subunits. 18S maturation is finalized by cleavage at site D in the cytoplasm, whereas maturation of 5.8S and 25S occurs in multiple steps in the nucleus. 85% of transcripts are cleaved by RNase MRP before being processed by the Rat1/Xrn1 complex and at site B_2. This is followed by cleavage at sites C_1 and C_2 and processing by Rex1 and Rex2 (van Hoof et al., 2000) and the exosome to generate mature 5.8S RNA. In the remaining 15% of transcripts, RNase MRP cleavage does not occur.

(B) Cartoon drawing of "Miller" spreads of actively transcribed rDNA genes (Miller and Beatty, 1969; Osheim et al., 2004). Preribosomes, shown as black globular entities, form at the 5′ end of the nascent transcript in a U3 snoRNA-dependent manner (Dragon et al., 2002). U3 snoRNA forms several short duplexes with pre-rRNA (Beltrame et al., 1994; Beltrame and Tollervey, 1992, 1995). Bms1 (red) and Rcl1 (green) are part of preribosomes (Grandi et al., 2002; Wegierski et al., 2001).

(C) Domain organization of Bms1. A GTPase domain of the Ras superfamily (red) is located at the N terminus (Sanchez and Sali, 1998). The binding sites for U3 snoRNA and Rcl1 are shown in cyan and green, respectively. The C-terminal portion of the protein, which is missing after proteolysis and in our expression construct Bms1(1–705), is shown in blue, separated from the rest of the protein by a flexible linker. The black lines indicate a bipartite nuclear localization signal (NLS). Protein regions of undefined function are shown in gray.

efficiently proteolyzed both in *E. coli* and in *S. cerevisiae*, a truncated construct, Bms1(1–705), comprising almost two-thirds of the native protein and designed according to the observed size and sequence of the major proteolysis fragment, could be stably expressed as an N-terminal maltose binding protein (MBP) fusion in bacteria. Unless otherwise stated, this construct, Bms1(1–705), was used in the experiments described below.

Bms1 Is a GTPase

To test whether Bms1 functions as a GTPase as suggested by sequence homology, we employed a standard hydrolysis assay by using γ-^{32}P-labeled GTP (Mohr et al., 2002; Peluso et al., 2001). Upon GTP hydrolysis, γ-^{32}P-GTP is converted to $^{32}P_i$ and GDP, which can be separated by thin-layer chromatography. Addition of 5 μM Bms1 increases the rate of GTP hydrolysis by 100-fold over the uncatalyzed rate (Figure 2A), similar to other GTPases (see Table S1 in the Supplemental Data available with this article online), and this activity copurified with Bms1 over three columns (data not shown), suggesting that the activity comes from Bms1 and not a contaminant. Additionally, GTPase activity is influenced by the addition of Rcl1 and U3 snoRNA, binding partners of Bms1 (see below), and the binding affinities obtained in GTPase and RNA binding experiments agree quantitatively (K.K. and J.A.D., unpublished data).

To rule out that the observed GTPase activity arises from a contaminant, we analyzed two point mutants of Bms1. One mutant, Bms1-7, has three amino acids in the Rcl1 binding region replaced with alanines (aa 557–559), which results in ~10- to 15-fold weaker binding to Rcl1 (Figure S1A and data not shown). Consequently, the GTPase activity of this mutant does not respond to

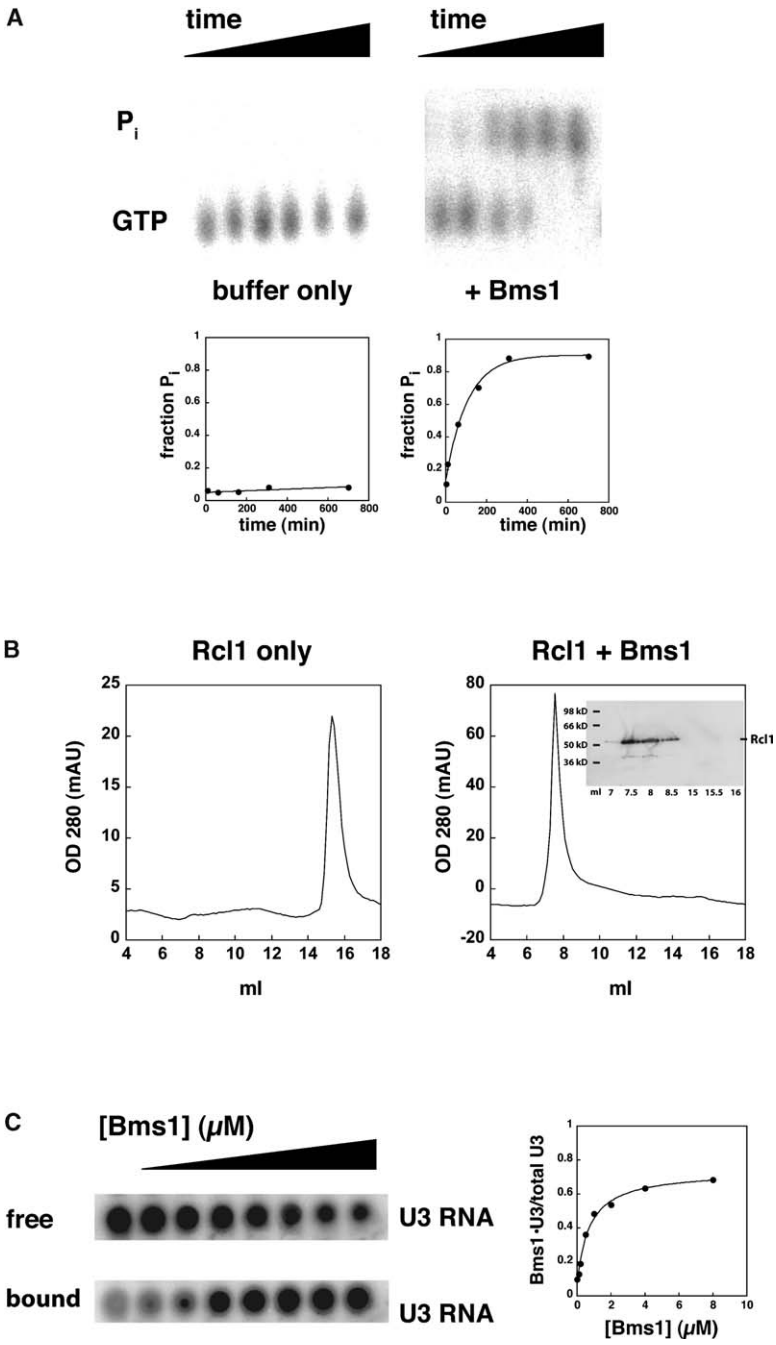

Figure 2. Biochemical Activities of Bms1

(A) GTPase assay. Autoradiogram of a TLC plate on which GTPase reactions were spotted (top), and quantitation of the autoradiogram (bottom) are shown. TLC plates were developed in 1 M LiCl and 300 mM NaH_2PO_4 (pH 3.8). Trace γ-^{32}P-GTP was incubated in the absence (left) or presence (right) of 5 μM Bms1. Time courses were fit to Equation 3 and yielded rate constants of 5×10^{-5} min^{-1} and 5.3×10^{-3} min^{-1} in the absence and presence of Bms1, respectively.

(B) Size-exclusion chromatography. Profile of Rcl1 on a Superdex 200 10/30 gel-filtration column in the absence (left) and presence (right) of Bms1 is shown. The column was run at 4°C. The insert shows a Western blot analysis for Rcl1.

(C) Nitrocellulose filter binding assay. An autoradiogram of a filter binding experiment to test binding of Bms1 to radiolabeled U3 snoRNA is shown on the left. The top row shows the Hybond N membrane, which retains unbound nucleic acid; and the bottom row shows the Hybond ECL nitrocellulose membrane, which retains protein and protein bound nucleic acid. Quantitation of the filter binding experiment is shown on the right. Data were fit with Equation 5 and yielded K_d = 0.7 μM.

the addition of Rcl1 as the wild-type protein does (Figure S1B and Figure 3A). The second mutant, Bms1(K82A), contains an alanine in place of lysine 82, which is part of the guanine binding pocket. In some GTPases, this lysine directly contacts the nucleotide. Analysis of the K82A mutant in vivo has shown that GTP binding of Bms1 in crude extracts is diminished (Gelperin et al., 2001). In agreement with these findings, we observe that GTP binding by Bms1(K82A) is weakened to 390 ± 30 μM (Figure S1C). In contrast, binding of GTP to wild-type Bms1 is ~200 μM (Figure 3A). Taken together, these data demonstrate that the GTPase activity measured in these assays arises from Bms1 and not from a contaminating *E. coli* protein.

Bms1 Binds Rcl1

A two-hybrid interaction between Bms1 and Rcl1 and copurification of Bms1 with tandem affinity purification (TAP)-tagged Rcl1 suggested that Bms1 binds directly to Rcl1 in vivo (Grandi et al., 2002; Krogan et al., 2004; Wegierski et al., 2001). To test this directly, samples of purified Bms1 (126 kDa) and Rcl1 (40 kDa) were analyzed by size-exclusion chromatography either individually or after incubation together for 1 hr on ice. In the presence of Bms1, Rcl1 elutes in an earlier fraction from the gel-filtration column, suggesting that Bms1 and Rcl1 bind in vitro in the absence of any accessory factors (Figure 2B). This interaction is specific, as Imp4p, another protein involved in ribosome biogenesis (Lee and Baserga,

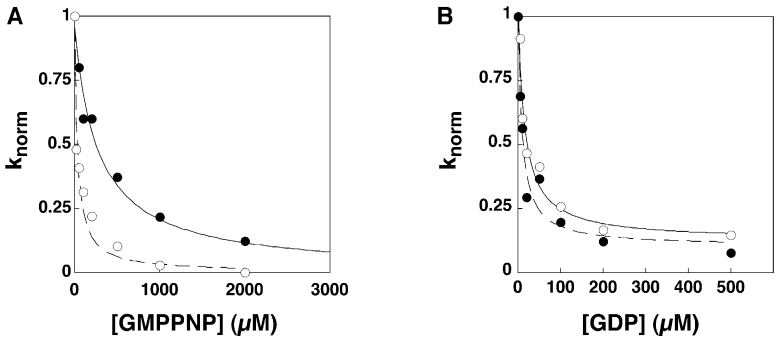

Figure 3. Effect of GMPPNP on Bms1's Affinity for Rcl1

(A) Binding affinity for the nonhydrolyzable GTP analog GMPPNP determined in inhibition experiments. Experiments were performed at 30ºC in the presence (○) and absence (●) of 4.7 μM Rcl1. Data were normalized and fit with Equation 4 to yield binding constants of 34 μM and 274 μM in the presence and absence of Rcl1, respectively. Error analysis of repeated experiments gives values for GMPPNP binding of 182 ± 88 and 14 ± 8 μM in the absence and presence of Rcl1, respectively. Increasing the Rcl1 concentration to 20 μM did not increase the size of the effect on GMPPNP binding (data not shown).

(B) Binding affinity for GDP, determined as above in the presence (○) and absence (●) of 4.7 μM Rcl1. Data were normalized and fit with Equation 4 and yielded binding constants of 10 μM and 16 μM in the presence and absence of Rcl1, respectively. Error analysis of repeated experiments gives values for GDP binding of 22 ± 10 and 14 ± 7 μM in the absence and presence of Rcl1, respectively.

1999), or Bms1-7, containing three mutations in the Rcl1 binding region, did not elicit a change in the gel-filtration behavior of Rcl1 (Figure S1A and data not shown). Because Rcl1 binding affects the GTPase activity of Bms1 (see below), we also conclude that this interaction is functional.

Bms1 Binds U3 snoRNA

Although Bms1 does not contain recognizable RNA binding motifs, we wondered whether it might nonetheless interact directly with U3 snoRNA. Consistent with this idea, recent work has uncovered RNA binding properties among proteins associated with U3 snoRNA in preribosomes, even though these proteins have no previously known RNA binding motifs (Steiner-Mosonyi et al., 2003; Wehner and Baserga, 2002; Eisenhaber et al., 2001; Gerczei and Correll, 2004). Additionally, or alternatively, known RNA binding motifs may have highly divergent primary sequences. Incubation of radioactively labeled U3 snoRNA with Bms1 resulted in Bms1-concentration-dependent retention of the RNA on the nitrocellulose in a filter binding experiment (Figure 2C). To show that RNA binding arose from Bms1 and not a contaminant, we performed a deletion analysis of Bms1. Bms1(1–182), which includes only the GTPase domain, does not bind U3 snoRNA (Figures S2A and S2B). Similarly, Bms1(1–315) and Bms1(1–448) fail to bind U3 snoRNA (Figures S2A and S2B). In contrast, Bms1 (1–482) binds RNA with an affinity of 2.5 μM (Figures S2A and S2B), comparable to Bms1(1–705). In contrast to these differences in RNA binding, all of these proteins hydrolyze GTP with comparable rate constants (data not shown), implying that the fragments are correctly folded. This analysis suggests that Bms1's RNA binding activity resides in the region between amino acids 448 and 482. Furthermore, because the U3 snoRNA binding affinity changes in response to changes in the Bms1 protein, this analysis also shows that RNA binding arises directly from Bms1 and not a contaminant.

To test whether binding of Bms1 to U3 snoRNA is specific, Bms1 protein was incubated with fragments of 25S and 18S rRNA as well as with 4.5S RNA (Figure S2C). As detected by retention of protein-RNA complexes on nitrocellulose filters, Bms1 recognizes only U3 snoRNA. Furthermore, competition experiments show that an excess of cold U3 snoRNA, but not a fragment of 18S rRNA or 4.5S RNA, can compete with U3 snoRNA for binding to Bms1 (Figure S2D). Although these data suggest that binding of U3 snoRNA to Bms1 may be specific, they also show that binding is weak. Thus, we cannot exclude the possibility that Bms1 binds other RNAs because the affinities of other complexes could be beyond the limit of detection by our assay. It is worth noting that U3 snoRNA is abundant in vivo (estimated [U3 snoRNA] $\geq$ 1 μM; K.K., J. Lee, and J.A.D., unpublished data), so evolution of a higher affinity binding interaction with Bms1 may not have been necessary.

Binding of GTP but Not GDP Increases Bms1- Rcl1 Interaction Affinity

GTPases are known to act as molecular switches that exhibit distinct behavior in their GDP and GTP bound forms. For example, in the GTP bound form the α subunit of heterotrimeric G proteins dissociates from the $\beta\gamma$ subunits, leading to pathway activation; the bacterial translation factor EF-Tu binds 100-fold more strongly to tRNA in its GTP bound form than in its GDP bound form (Pingoud et al., 1982; Pingoud and Urbanke, 1980; Romero et al., 1985). Thus, we wanted to test whether Bms1 binding to Rcl1 was similarly influenced by the nucleotide bound state of Bms1.

Because the gel-filtration assay shown in Figure 2B was not fully quantitative, possibly due to loss of Rcl1 protein on the tube walls at very low concentrations (data not shown), we had to use an alternate method to measure the affinity of Bms1 to Rcl1 in the presence and absence of GMPPNP. This strategy is outlined in Figure 4 and takes advantage of the fact that binding energy is conserved regardless of the way a complex is assembled (see Lorsch and Herschlag, 1998; McConnell et al., 1993; Shan and Herschlag, 1996 for applications of this strategy in other systems). For Bms1-GTP-Rcl1 complex formation, the free energy in going from free Bms1 to Bms1-GTP-Rcl1 is the same regardless of whether Rcl1 or GTP binds first (see Equation 1, derived from the scheme depicted in Figure 4).

$$K_{d,\mathrm{Rcl1}} \cdot K_{d,\mathrm{GTP}^*} = K_{d,\mathrm{GTP}} \cdot K_{d,\mathrm{Rcl1}^*} \quad (1)$$

In other words, the relationship between Bms1-Rcl1 affinity in the presence and absence of GTP is the

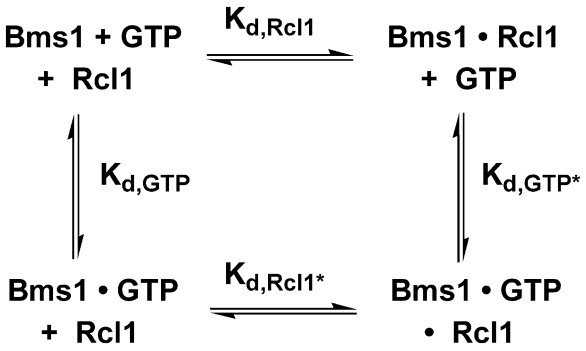

Figure 4. Thermodynamic Box Describing the Relationship between the Affinities for GTP in the Absence and Presence of Rcl1 and the Affinity for Rcl1 in the Absence and Presence of GTP

same as the relationship between Bms1-GTP affinity in the presence and absence of Rcl1 (Equation 2, derived from Equation 1).

$$K_{d,Rcl1}/K_{d,Rcl1*} = K_{d,GTP}/K_{d,GTP*} \quad (2)$$

Thus, to determine whether Bms1 binds Rcl1 more strongly in the presence of GTP than in its absence, we compared its affinity for GTP in the presence and absence of Rcl1 (Equation 2).

Bms1 binds GTP weakly (K_d ~200 μM, Figure 3A). Thus, GTP affinity could not be determined directly by varying the Bms1 concentration, as sufficiently high Bms1 concentrations could not be obtained. Instead, we measured the affinity for GMPPNP, a nonhydrolyzable GTP analog (e.g., Peluso et al., 2000; Rodnina et al., 1997) that can be used at concentrations high enough to saturate binding (see below).

To learn if Bms1 binding to Rcl1 was strengthened when GMPPNP (or GTP) was bound, we compared Bms1's affinity for GMPPNP in the presence and absence of Rcl1. Figure 3A shows that Rcl1 binding to Bms1 increases Bms1 affinity for GMPPNP ~10-fold. As described above, this finding means that GTP binding increases the affinity for Rcl1. In contrast, Rcl1 had no effect on binding of GDP (Figure 3B). Thus, GTP hydrolysis (and conversion to GDP) reduces the affinity for Rcl1.

Rcl1 Association Increases Bms1-U3 snoRNA Binding Affinity

To test whether Rcl1 binding to the preformed Bms1-GMPPNP complex affects binding to U3 snoRNA, we determined the U3 snoRNA affinity for the Bms1-GMPPNP complex in the presence and absence of Rcl1. Using nitrocellulose filter binding as before, the data show that Bms1-GMPPNP binding to U3 snoRNA is strengthened ~5-fold in the presence of Rcl1 (Figure 5A). This suggests that binding of Rcl1 helps binding of the Bms1-GTP complex to U3 snoRNA and its associated preribosomes.

To test whether GTP hydrolysis and concomitant dissociation of Rcl1 would lead to dissociation of Bms1 from U3, we determined the affinity of Bms1-GDP for U3 snoRNA in the presence and absence of Rcl1. Dissociation of Rcl1 from the Bms1-GDP complex weakens binding to U3 snoRNA ~3-fold (Figure 5B).

The C-Terminal Domain of Bms1 Acts as an Intramolecular GTPase Activator

GTPases typically have low intrinsic GTPase activity, which is stimulated upon interaction with a specific GTPase-activating protein (GAP) to achieve tight spatial and temporal control of GTP-regulated activity (Bourne et al., 1991). To test whether truncation of its C terminus affected Bms1 activity, we performed control experiments with full-length Bms1. Although overexpression was poor and stability severely limited (<1 week), thereby preventing routine use of full-length Bms1, enough material was obtained to do control experiments. Surprisingly, these experiments revealed that full-length Bms1 was a better GTPase than Bms1(1–705) (Figure 6). In side-by-side experiments performed with protein prepared in parallel, full-length Bms1 hydrolyzed GTP ~8-fold faster than Bms1(1–705). Nevertheless, both proteins bound GDP and GMPPNP with the same affinity (Table S2), suggesting that the GTP binding site was not affected. Furthermore, both proteins bind U3 snoRNA with similar binding constants (Table S2), suggesting that the difference in GTPase activity is not due to fewer active molecules in the Bms1(1–705) preparation relative to full-length Bms1. (Note that the slightly higher K_d value for full-length Bms1 suggests that the

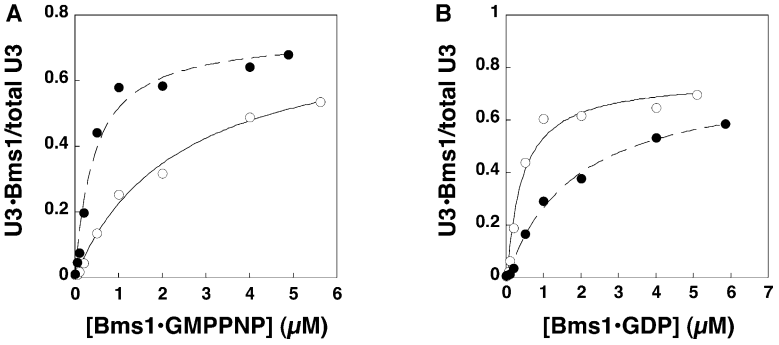

Figure 5. Effect of Rcl1 Binding to Bms1 on Affinity for U3 snoRNA

(A) Affinity for U3 snoRNA to Bms1-GMPPNP in the presence (●) or absence (○) of 8.9 μM Rcl1 is shown. The GMPPNP concentration was 1.75 mM. Data were fit with Equation 5 and yielded binding constants of 0.4 μM and 2.4 μM in the presence (●) and absence (○) of Rcl1, respectively. Error analysis of repeated experiments gives values for U3 snoRNA binding of 2.2 ± 1.7 and 0.4 ± 0.2 μM in the absence and presence of Rcl1, respectively.

(B) Effect of Rcl1 dissociation from Bms1•GDP on affinity for U3 snoRNA. The affinity for U3 snoRNA to Bms1-GDP in the presence (●) or absence (○) of 8.9 μM Rcl1 is shown. The GDP concentration was 1.1 mM. Data were fit with Equation 5 and yielded binding constants of 0.4 μM and 2.0 μM in the presence (●) or absence (○) of Rcl1, respectively. Error analysis of repeated experiments gives values for U3 snoRNA binding of 1.5 ± 0.5 and 0.7 ± 0.2 μM in the absence and presence of Rcl1, respectively.

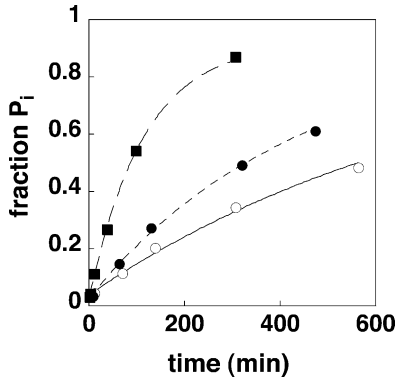

Figure 6. Effect of the C-Terminal Domain of Bms1 on GTPase Activity

Time course for GTP hydrolysis by 1 μM full-length Bms1 (■), Bms1(1–705) (○), or Bms1(1–855) (●) is shown. Data were fit with Equation 3 and yielded rate constants of 8.7×10^{-3} min^{-1}, 1.3×10^{-3} min^{-1}, and 2.3×10^{-3} min^{-1}, respectively.

protein concentration overestimates the number of active molecules, which would lead to an even more significant stimulation of the GTPase activity). Interestingly, a Bms1 variant lacking just the C-terminal domain homologous to dynamin's internal GAP domain, Bms1(1–855), hydrolyzes GTP with rates similar to Bms1(1–705) (see Figure S3 and Discussion). It has not been possible to express the C-terminal domain of Bms1 independently to test whether it can provide GAP activity in *trans*.

A Mutant Bms1 Protein that Cannot Bind Rcl1 Results in Loss of Binding of Rcl1 to Preribosomes In Vivo

To test the effects of Bms1 mutations in vivo, we constructed a yeast strain with a galactose-inducible promoter to shut off expression of endogenous Bms1 at desired times by the addition of glucose. In the presence of glucose, this strain continues to grow only when transformed with a plasmid encoding wild-type Bms1 (Figure 7A, and data not shown). To test the effect of mutations in Bms1, plasmids were introduced into this strain that encoded no protein, wild-type Bms1, or Bms1(ΔRcl1), which contains a deletion of the Rcl1 binding site (amino acids 536–559). Although not affecting its GTPase activity or folding as assessed by CD-spectroscopy, this deletion weakens Bms1 binding to Rcl1 by ~40-fold (data not shown).

We first determined whether deletion of the Rcl1 binding site affected yeast-cell growth. After 15 hr in the presence of glucose, cells without Bms1 (Figure 7A, open circles) grow more slowly than cells with wild-type Bms1 (Figure 7A, closed circles). Cells expressing Bms1(ΔRcl1) continue to grow with an ~2-fold-slower growth rate (doubling times are 1.8, 6.3, and 3.3 hr for wild-type Bms1, no Bms1, or Bms1[ΔRcl1], respectively).

To test whether Rcl1 binding to preribosomes requires binding to Bms1, we performed a density-gradient analysis as described previously (Billy et al., 2000; Wegierski et al., 2001). Extracts from yeast cells grown in glucose and transformed with plasmids encoding no protein,

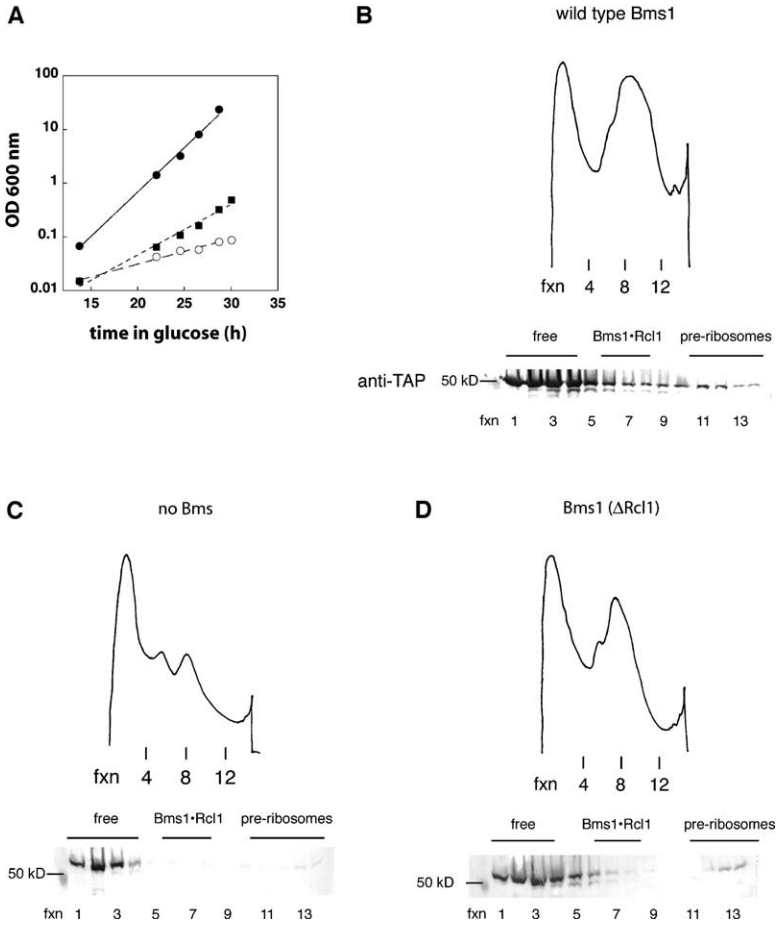

Figure 7. Growth Curves

(A) Growth of yeast cells was determined after endogenous Bms1 was depleted and cells were supplied with a plasmid with wild-type Bms1 (●), without insert (○), or with Bms1(ΔRcl1) (■).

(B–D) Gradient analysis of preribosomes from cells with wild-type Bms1 (B), without Bms1 (C), and with Bms1(ΔRcl1) (D). Cell extracts were loaded on a 10%–30% glycerol gradient spun for 5 hr at 36,000 rpm. 750 μl fractions were collected and the OD was measured at 260 nm (top). Presence of Rcl1 was tested by Western blotting analysis with an antibody against the TAP-tag on Rcl1 (bottom). Fractions reflecting free Rcl1, Bms1-bound Rcl1, and Rcl1 in preribosomes are indicated (Gelperin et al., 2001; and data not shown).

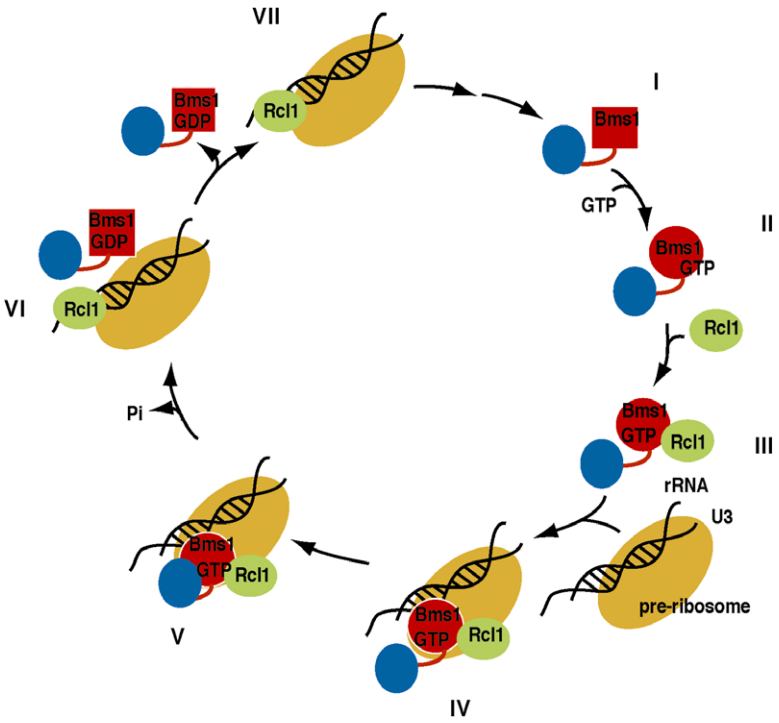

Figure 8. Model for the Function of Bms1 in Ribosome Biogenesis

The N-terminal domain of Bms1, which includes the GTPase domain, is shown in red and its C-terminal domain is shown in blue. These domains are linked by a flexible tether, which is shown in red. Rcl1 is shown in green. Preribosomes are shown in orange and U3 is shown in a duplex with pre-rRNA. GTP binding increases the affinity for Rcl1, leading to formation of a ternary complex of Bms1-GTP and Rcl1. This complex binds tightly to U3 snoRNA, which is bound to pre-rRNA, locating the complex to preribosomes. A conformational change within Bms1 may activate its GTPase activity by promoting interaction between the GTPase and the GAP domain. Dissociation of Rcl1 from GDP bound Bms1 leads to dissociation of Bms1-GDP from U3 snoRNA.

wild-type Bms1, or Bms1(ΔRcl1) were applied to 10%–30% glycerol gradients to separate free Rcl1 from Rcl1 bound to Bms1, which forms a previously characterized 10S complex (Wegierski et al., 2001), and from Rcl1 bound to preribosomes (Figures 7B–7D).

As shown previously in strains with wild-type Bms1, Rcl1 can be found in three distinct areas of the glycerol gradient (Figure 7B). Most Rcl1 is free and remains on top of the gradient. A significant fraction of Rcl1 is bound to Bms1 and sediments in the intermediate portion of the gradient, whereas the remaining Rcl1 is found at the bottom of the gradient, bound to preribosomes. When cells are depleted of Bms1 and supplemented only with a plasmid encoding no protein, only free Rcl1 is observed (Figure 7C). As expected, in cells in which Bms1(ΔRcl1) is the only expressed form of Bms1, Rcl1 is no longer found in the fraction bound to Bms1. Interestingly, in these cells, the amount of Rcl1 bound to preribosomes is also substantially reduced, consistent with the idea that Bms1 binding is required to recruit Rcl1 to preribosomes.

Discussion

A Model for Bms1 Function in Ribosome Biogenesis

We have used quantitative biochemical analysis to delineate the function of Bms1, an essential GTPase involved in ribosome biogenesis. Our experiments show that Bms1 directly binds Rcl1, an essential protein involved in ribosome biogenesis (Figure 2B), consistent with previous in vivo data (Krogan et al., 2004; see also Wegierski et al., 2001). In addition, we find that Bms1 binds to U3 snoRNA (Figure 2C).

The interdependence of these activities, analyzed by using purified Bms1, Rcl1, and in vitro-transcribed U3 snoRNA, shows thermodynamic coupling in binding of GTP, Rcl1, and U3 snoRNA to Bms1. These results suggest a model for the roles of Bms1 and Rcl1 in preribosome complex assembly (Figure 8). The GTPase cycle of Bms1 starts with association of GTP. Because GTP binding increases the affinity of Bms1 for Rcl1, we hypothesize that a conformational rearrangement occurs within Bms1, symbolized by the shape change from a rectangle to a circle in Figure 8 (I→II). Rcl1 then associates with this conformation of Bms1 (Figure 8, II→III). We have shown that binding of Rcl1 increases the affinity of the Bms1-GTP complex for U3 snoRNA. The next step in the GTPase cycle of Bms1 is binding of the Bms1-GTP-Rcl1 complex to preribosomes via interaction with U3 snoRNA (Figure 8, III→IV). The C-terminal domain of Bms1 stimulates its GTPase activity without affecting its affinity for U3 snoRNA or GTP. Furthermore, its linker is susceptible to proteolysis and contains a region of low complexity (data not shown), suggesting that it is flexible. We thus speculate that a signal on the preribosome may induce a conformational change about this linker that brings the C-terminal domain toward the N-terminal domain (Figure 8, IV→V), leading to GTP hydrolysis in the next step (V→VI). Because GTP, but not GDP binding, increases Bms1-Rcl1 affinity, GTP hydrolysis contributes to the release of Rcl1 (Figure 8, V→VI), perhaps onto the preribosomes (Figure 8, complex VI). Because GDP bound Bms1 binds U3 snoRNA with low affinity, release of Rcl1 is expected to facilitate dissociation of Bms1-GDP from preribosomes (Figure 8, VI→VII).

Consistent with this model, in vivo data demonstrate that binding to Rcl1 is an important function of Bms1, because deletion of the Rcl1 binding site leads to a reduction in the growth rate close to the background of the Bms1 deletion. The residual slow growth rate may be due to residual binding of Bms1 to Rcl1 or due to the ability of Rcl1 to bind to preribosomes by itself (Figure 7D and see below). As shown previously (Wegierski

et al., 2001), Rcl1 can be found free, bound to Bms1, and bound to the preribosomes. As also shown previously, depletion of Bms1 (but not Imp3p, another protein involved in ribosome biogenesis [Wegierski et al., 2001]) leads to loss of copurification of Rcl1 in complex with Bms1 and with preribosomes. Here, we have shown that in Bms1(ΔRcl1) cells, Rcl1 is not observed to associate with Bms1. Furthermore, the Rcl1 fraction bound to preribosomes is significantly depleted, as expected for a model in which Bms1 delivers Rcl1 to preribosomes. The residual small amount of Rcl1 bound to preribosomes may reflect binding of Rcl1 to preribosomes independent of Bms1 or residual binding of Rcl1 to Bms1(ΔRcl1). This residual amount of Rcl1 can also explain the remaining slow growth of the Bms1(ΔRcl1) cells.

Taken together, our data provide evidence for a series of thermodynamically coupled binding events in which Bms1 is a GTP-controlled vehicle for depositing Rcl1 on preribosomes. This model is consistent with the low amount of Rcl1 found on preribosomes in the Bms1(ΔRcl1) cells (Figure 7D). Once delivered by Bms1, Rcl1 could be kinetically trapped on preribosomes, performing its function faster than it dissociates. Such an effect has been previously observed with the exon junction complex, which is deposited upstream of the 5′-splice site in pre-mRNAs and remains bound at this location until nuclear export is completed but cannot bind in the absence of splicing (Kataoka et al., 2000; Le Hir et al., 2000).

The C-Terminal Domain Acts as an Intramolecular GAP

All GTPases have specific GTPase-activating proteins (GAPs) that accelerate their GTPase activity between 5- and 10^6-fold (Table S1). The data presented here show that full-length Bms1 is a better GTPase than the truncated Bms1(1–705) or Bms1(1–855) (Figure 6), even though GTP binding and RNA binding activities are not affected. This suggests that the C-terminal domain constitutes an intramolecular GAP, perhaps explaining in part the unusually large size of Bms1 relative to other GTPases (Bms1, 136 kDa; Ras, 34 kDa; EF-Tu, 50 kDa).

Interestingly, an internal GAP domain has been demonstrated within dynamin, a GTPase essential for clathrin-mediated endocytosis (Song and Schmid, 2003). Assembly of dynamin tetramers into higher-order structures increases the GTPase activity 5- to 10-fold, whereas microtubule- or lipid-mediated assembly increases GTPase activity 50- to 100-fold (Narayanan et al., 2005; Tuma et al., 1993; Warnock et al., 1996). Kinetic studies have shown that a 13 kDa domain within dynamin is responsible for this effect and acts as an intramolecular GAP (Muhlberg et al., 1997). Notably, the C-terminal domain of Bms1 is 16% identical and 35% similar in sequence to the GAP domain of dynamin (Figure S3).

Similarities to Other GTPase-Controlled Steps on the Ribosome

The proposed GTPase-controlled delivery of Rcl1 to preribosomes by Bms1 is reminiscent of the delivery of tRNAs to translating ribosomes by the EF-Tu GTPase. Similar to the results described above, EF-Tu binds tRNA tighter in the presence of GTP than in the presence of GDP (Pingoud et al., 1982; Pingoud and Urbanke, 1980; Romero et al., 1985), leading to loading of aminoacylated tRNA (aatRNA) to the GTP bound state. After initial binding and codon recognition, EF-Tu's GTPase is activated, leading to dissociation of EF-Tu, whereas the aatRNA remains bound for peptidyl transfer (Rodnina and Wintermeyer, 2001). Interestingly, the sequence of Bms1 is more homologous to elongation factors than to other GTPases (Sanchez and Sali, 1998; Wegierski et al., 2001). Likewise, protein folds found in ribosomal proteins or translation factors occur in proteins involved in ribosome biogenesis, and there is considerable functional overlap of these proteins as well (e.g., Basu et al., 2001; Dunbar et al., 2000; Lee and Baserga, 1999; Palm et al., 2000; Venema and Tollervey, 1996). This structural and functional conservation might reflect a common evolutionary origin, suggesting that the complex eukaryotic ribosome biogenesis apparatus was adapted from the translational machinery.

Experimental Procedures

Materials

GTP, GMPPNP (guanosineimidodiphosphate), and GDP were purchased from Sigma and were fast-pressure liquid chromatography (FPLC) purified using a Mono Q column (Amersham). Nucleotides were adsorbed to the column matrix in a solution of 50 mM $(NH_4)HCO_3$ (pH 8.0) and eluted with a salt gradient to 1 M $(NH_4)HCO_3$. Peak fractions were lyophilized twice and show no remaining contamination. Purified nucleotides were dissolved in water and aliquots were flash frozen and stored at −80ºC. γ-^{32}P-GTP was purchased from Amersham, purified on a 24% acrylamide gel with TBE buffer, eluted overnight with water, and stored at −20ºC.

Cloning

Bms1 and Rcl1 as well as U3 snoRNA were cloned from genomic yeast DNA by polymerase chain reaction (PCR) amplification of the respective gene. Bms1 was cloned between the SfoI and HindIII sites of vector pSV272 (a gift from J. Berger, University of California, Berkeley) to produce plasmid pKK101. This introduces an N-terminal maltose binding protein (MBP)-tag, cleavable with tobacco etch virus (TEV) protease. Plasmid pKK102, which contains Bms1(1–705) in the same vector above, was created by PCR using a primer that introduces a premature stop codon. Rcl1 was cloned between the NotI and NdeI sites of pET17b (Novagen) to produce plasmid pKK130. Protein expression from this plasmid yields untagged protein. U3 snoRNA and other RNAs were cloned between the PstI and XmaI sites of plasmid pUC19 (New England Biolabs) with the addition of a BtsI restriction site at the 3′ end for linearization prior to transcription to produce a native 3′ end. Please refer to Table S3 for oligonucleotides used in this study.

For transformations into yeast, wild-type Bms1 or Bms1(ΔRcl1) was cloned between the XhoI and SacII sites of pRS315 to give plasmids pKK301 and pSJ314, respectively.

Transcriptions

Transcriptions were performed in the presence of 40 mM Tris (pH 8.1), 25 mM $MgCl_2$, 2 mM spermidine, 0.01% Triton X-100, 2 mM of each NTP, 40 mM DTT, 0.5 mg T7 RNA polymerase, and 200 μg template per each 10 ml reaction. After transcription, RNA was purified by using RNeasy columns (Qiagen) or denaturing polyacrylamide gels. Radioactively labeled RNA was obtained by transcriptions in the presence of 50 μCi α-^{32}P-ATP (Amersham), essentially as described above, except that 0.2 mM ATP and 1 μg template/50 μl reaction was used. Transcripts were purified on a 6% TBE (Tris-borate-EDTA) polyacrylamide gel in the presence of 8 M urea. RNA was eluted from the gel with an Elutrap gel-electroelution device (Schleicher & Schuell) and stored in TBE at −20ºC.

Protein Expression

For expression of the Bms1 protein, plasmid DNA was freshly transformed into Rosetta cells (Novagen). Overnight cultures were used

to inoculate fresh LB medium containing 12.5 μg/l kanamycin and 34 μg/l chloramphenicol. Cells were grown at 37ºC to an OD of 0.4, induced by the addition of IPTG (final concentration 0.1 mM), and shifted to 30ºC, where they were grown for an additional 4 hr.

For expression of Rcl1 protein, plasmid DNA was transformed into BL21(DE3) cells and grown in the presence of 100 μg/ml ampicillin; induction was performed as described above.

Protein Purification

For purification of Bms1, cells from a three-liter culture were resuspended in 100 ml of buffer A (50 mM NaH_2PO_4 [pH 8.0], 300 mM NaCl, 1 M KCl, 2 mM EDTA) supplemented with 0.5 mM PMSF and two tablets of protease inhibitor (Roche). The suspension was sonicated, and cell debris was pelleted. The supernatant was loaded onto a gravity-flow column containing 4 ml amylose resin (New England Biolabs). The column was washed with 20 ml of buffer A and with 30 ml of buffer B (50 mM NaH_2PO_4 [pH 8.0], 300 mM NaCl, 2 mM EDTA). Protein was eluted in 25 ml buffer C (50 mM NaH_2PO_4 [pH 8.0], 300 mM NaCl, 10 mM maltose, and 2 mM EDTA) and concentrated for loading onto a Superdex 200 column. The gel-filtration column was run in a buffer containing 200 mM KCl, 50 mM HEPES (pH 7.7), 1 mM DTT, 1 mM TCEP (Tris(2-carboxyethyl)phosphine hydrochloride, BioVectra, Oxford, CT). Purity was >98% (Figure S4), with the main contaminating bands being proteolysis fragments of Bms1 according to mass spectrometry. Typical yields were 1 mg and 0.25 mg for Bms1(1–705) and full-length Bms1, respectively. Protein was stored at 4ºC for 2 to 3 weeks and <1 week for Bms1(1–705) and full-length Bms1, respectively. Control experiments with Bms1(1–705) after removal of the MBP tag by protease cleavage showed that the tag does not interfere with GTPase activity or RNA binding (data not shown). However, because removal of the MBP-tag rendered the protein more susceptible to proteolysis (data not shown), the affinity tag was not routinely removed.

For purification of Rcl1, cells from 3 liters of medium were resuspended in 50 ml of 50 mM Hepes (pH 7.7) supplemented with one tablet of protease inhibitor. Cell debris was pelleted, and the supernatant was applied at 1 ml/min to a 5-ml Fast-Flow S column (Amersham). Protein was eluted in a salt gradient to 1 M NaCl over 10 column volumes. Peak fractions were pooled and concentrated for injection onto a Superdex 75 column, which was run in 200 mM KCl, 50 mM Hepes, 10% glycerol, and 1 mM DTT. The peak fractions from the Superdex 75 column were analyzed for GTPase contamination, and protein was flash frozen in liquid nitrogen for long-term storage at −80ºC. Typical yields were 40 mg without visible contamination (Figure S4). Rcl1 is stable at –80ºC for at least 1 year.

Protein concentrations were determined by the Bradford method using a BSA standard curve, which agrees well with sodium dodecyl-sulfate-polyacrylamide gel electrophoresis (SDS-PAGE) quantification.

Rcl1 and Bms1 binding assays were used to determine the fraction of active molecules. Assuming a 1:1 stoichiometry (as indicated from kinetic, RNA binding, and gel-filtration experiments), these experiments suggest that >90% of Rcl1 molecules are active and >60% of Bms1 molecules are active.

GTPase Assays

GTPase assays were performed at 30ºC in the presence of 10 mM $MgCl_2$, 200 mM KCl, and 50 mM Hepes (pH 7.7). For single-turnover experiments, a trace amount (< 1 nM) of γ-^{32}P-GTP was mixed with $MgCl_2$ and used to initiate reactions. Time points were quenched by the addition of an equal volume of 0.75 M KH_2PO_4 (pH 3.3) (Peluso et al., 2001). One microliter of the quenched reaction was spotted onto a PEI-F cellulose TLC plate (J.T. Baker), which had been washed with 10% NaCl and twice with water. The TLC plate was developed in a 1 M LiCl and 300 mM NaH_2PO_4 (pH 3.8) solution (Peluso et al., 2001) and quantitated with a phosphorimager. These data were fit with Equation 3 to obtain rate constants, k_{obs}, for GTP hydrolysis.

$$fraction_{reacted} = fraction^{max}_{reacted} - fraction^{max}_{reacted} \bullet \exp(-k_{obs} \bullet t) \quad (3)$$

K_i Values

Inhibition constants for GDP and GMPPNP were obtained by using subsaturating concentrations of Bms1 (1–3 μM Bms1) and increasing concentrations of GDP or GMPPNP. At concentrations higher than 1 mM, an equal concentration of $MgCl_2$ was added to the reaction to account for chelation of Mg^{2+} by the nucleotide. The data were fit with Equation 4 to obtain K_i values.

$$k_{obs} = \frac{k_{max}}{1+\frac{[GDP]}{K_i}} \quad (4)$$

Reactions in the presence of Rcl1 were performed with 4–9 μM Rcl1, and reactions in the presence of Bms1 were performed with U3 snoRNA concentrations at least in 2-fold excess of Bms1 to ensure that all Bms1 has U3 snoRNA bound.

Nitrocellulose Filter Binding Assays

RNA was prefolded by incubation for 20 min at 55ºC in the presence of 10 mM $MgCl_2$ and 50 mM Hepes (pH 7.7), after which it ran as a single band in native gels and was able to bind Bms1 protein. Prefolded RNA was incubated for 2 hr with Bms1 protein at 30ºC in the presence of binding buffer (10 mM $MgCl_2$, 50 mM Hepes [pH 7.7], and 200 mM KCl). Varying the incubation time to 5 hr had no appreciable influence on the K_d values obtained, suggesting that binding has come to equilibrium (data not shown). This was further corroborated by measuring dissociation rate constants. During incubation, the membranes for filter binding (Hybond-N, Hybond-ECF [both Amersham], and Tuffryn 0.45 μm filters [Pall Corporation]) were washed for 30 min in binding buffer. After all reactions were spotted, each spot was washed with 100 μl binding buffer and membranes were disassembled and exposed to a phosphorscreen. Bound and free RNA was quantitated by phosphorimager analysis, and the fraction of bound RNA was fit with Equation 5 to obtain K_d values.

$$fraction_{bound} = fraction^{max}_{bound}\frac{[Bms1]}{[Bms1]+K_d} \quad (5)$$

Error Analysis and Reproducibility

Variability between rate constants obtained with protein from different preparations was within less than 2-fold. Variability between binding constants obtained with different protein preparations was the same as variability between different days, which was <50% for both GDP/GMPPNP and U3 snoRNA binding. The ratios for GMPPNP/GDP and U3 snoRNA binding to different Bms1-containing complexes varied only <30% and <40% between experiments, respectively. Each data point was repeated at least four times. Over the course of this work, we used four different Rcl1 protein preparations, three U3 snoRNA preparations, and dozens of Bms1 preparations.

Construction of the Galactose-Inducible Bms1 Strain

The wild-type Bms1 promoter was replaced with a galactose-inducible promoter in the background of the Rcl1-TAP strain (Ghaemmaghami et al., 2003) using a KAN-marker as described (Longtine et al., 1998). Insertion at the correct genomic locus was verified by colony PCR. Furthermore, as expected because Bms1 is an essential protein (Gelperin et al., 2001; Wegierski et al., 2001; Winzeler et al., 1999), the Bms1:Gal strain did not grow on glucose-containing medium but is rescued by the addition of a Bms1-containing plasmid.

Gradient Analysis

Gradient analysis of preribosomes was performed as described (Billy et al., 2000; Wegierski et al., 2001). Cells were grown at 30ºC for ~30 hr in YPD to deplete endogenous Bms1 (data not shown and Figure 7A). During this time, cells were maintained in log phase by diluting at appropriate intervals. ~70×10^7 cells were harvested below OD 0.4. After glycerol gradient centrifugation, 750 μl fractions were collected and 200 μl were methanol precipitated and resuspended in 80 μl SDS loading buffer, 20 μl of which was loaded onto an SDS gel for probing with an anti-calmodulin antibody against the TAP-tag on Rcl1.

Supplemental Data

Supplemental Data including four figures, three tables, and supplemental references are available online with this article at http://www.molecule.org/cgi/content/full/20/4/633/DC1/.

Acknowledgments

This work was supported in part by National Institutes of Health grant GM22778. J.A.D. is a Howard Hughes Medical Institute investigator. K.K. is a Damon Runyon Fellow supported by the Damon Runyon Cancer Research Foundation (DRG-1807-04). S.J. was supported by a fellowship from the German National Academic Foundation. We thank K. Carroll, J. Gallagher, W. Gilbert, J. Hershey, and S. Shan for comments on the manuscript; and C. Fraser and J. Gallagher for experimental help and advice.

Received: May 23, 2005
Revised: August 12, 2005
Accepted: September 20, 2005
Published: November 22, 2005

References

Basu, U., Si, K., Warner, J.R., and Maitra, U. (2001). The Saccharomyces cerevisiae TIF6 gene encoding translation initiation factor 6 is required for 60S ribosomal subunit biogenesis. Mol. Cell. Biol. *21*, 1453–1462.

Beltrame, M., Henry, Y., and Tollervey, D. (1994). Mutational analysis of an essential binding site for the U3 snoRNA in the 5′-external transcribed spacer of yeast pre-ribosomal RNA. Nucleic Acids Res. *22*, 5139–5147.

Beltrame, M., and Tollervey, D. (1992). Identification and functional analysis of two U3 binding-sites on yeast pre-ribosomal RNA. EMBO J. *11*, 1531–1542.

Beltrame, M., and Tollervey, D. (1995). Base-pairing between U3 and the pre-ribosomal RNA is required for 18S ribosomal RNA synthesis. EMBO J. *14*, 4350–4356.

Billy, E., Wegierski, T., Nasr, F., and Filipowicz, W. (2000). Rcl1p, the yeast protein similar to the RNA 3′-phosphate cyclase, associates with U3 snoRNP and is required for 18S rRNA biogenesis. EMBO J. *19*, 2115–2126.

Bourne, H.R., Sanders, D.A., and McCormick, F. (1991). The GTPase superfamily: conserved structure and molecular mechanism. Nature *349*, 117–127.

Decatur, W.A., and Fournier, M.J. (2003). RNA-guided nucleotide modification of ribosomal and other RNAs. J. Biol. Chem. *278*, 695–698.

Dragon, F., Gallagher, J.E., Compagnone-Post, P.A., Mitchell, B.M., Porwancher, K.A., Wehner, K.A., Wormsley, S., Settlage, R.E., Shabanowitz, J., Osheim, Y., et al. (2002). A large nucleolar U3 ribonucleoprotein required for 18S ribosomal RNA biogenesis. Nature *417*, 967–970.

Dunbar, D.A., Dragon, F., Lee, S.J., and Baserga, S.J. (2000). A nucleolar protein related to ribosomal protein L7 is required for an early step in large ribosomal subunit biogenesis. Proc. Natl. Acad. Sci. USA *97*, 13027–13032.

Eisenhaber, F., Wechselberger, C., and Kreil, G. (2001). The Brix domain protein family—a key to the ribosomal biogenesis pathway? Trends Biochem. Sci. *26*, 345–347.

Fromont-Racine, M., Senger, B., Saveanu, C., and Fasiolo, F. (2003). Ribosome assembly in eukaryotes. Gene *313*, 17–42.

Gelperin, D., Horton, L., Beckman, J., Hensold, J., and Lemmon, S.K. (2001). Bms1p, a novel GTP-binding protein, and the related Tsr1p are required for distinct steps of 40S ribosome biogenesis in yeast. RNA *7*, 1268–1283.

Gerczei, T., and Correll, C.C. (2004). Imp3p and Imp4p mediate formation of essential U3-precursor rRNA (pre-rRNA) duplexes, possibly to recruit the small subunit processome to the pre-rRNA. Proc. Natl. Acad. Sci. USA *101*, 15301–15306.

Ghaemmaghami, S., Huh, W.K., Bower, K., Howson, R.W., Belle, A., Dephoure, N., O'Shea, E.K., and Weissman, J.S. (2003). Global analysis of protein expression in yeast. Nature *425*, 737–741.

Grandi, P., Rybin, V., Bassler, J., Petfalski, E., Strauss, D., Marzioch, M., Schafer, T., Kuster, B., Tschochner, H., Tollervey, D., et al. (2002). 90S pre-ribosomes include the 35S pre-rRNA, the U3 snoRNP, and 40S subunit processing factors but predominantly lack 60S synthesis factors. Mol. Cell *10*, 105–115.

Kass, S., Tyc, K., Steitz, J.A., and Sollner-Webb, B. (1990). The U3 small nucleolar ribonucleoprotein functions in the first step of preribosomal RNA processing. Cell *60*, 897–908.

Kataoka, N., Yong, J., Kim, V.N., Velazquez, F., Perkinson, R.A., Wang, F., and Dreyfuss, G. (2000). Pre-mRNA splicing imprints mRNA in the nucleus with a novel RNA-binding protein that persists in the cytoplasm. Mol. Cell *6*, 673–682.

Kiss, T. (2002). Small nucleolar RNAs: an abundant group of noncoding RNAs with diverse cellular functions. Cell *109*, 145–148.

Krogan, N.J., Peng, W.T., Cagney, G., Robinson, M.D., Haw, R., Zhong, G., Guo, X., Zhang, X., Canadien, V., Richards, D.P., et al. (2004). High-definition macromolecular composition of yeast RNA-processing complexes. Mol. Cell *13*, 225–239.

Le Hir, H., Moore, M.J., and Maquat, L.E. (2000). Pre-mRNA splicing alters mRNP composition: evidence for stable association of proteins at exon-exon junctions. Genes Dev. *14*, 1098–1108.

Lee, S.J., and Baserga, S.J. (1999). Imp3p and Imp4p, two specific components of the U3 small nucleolar ribonucleoprotein that are essential for pre-18S rRNA processing. Mol. Cell. Biol. *19*, 5441–5452.

Longtine, M.S., McKenzie, A., 3rd, Demarini, D.J., Shah, N.G., Wach, A., Brachat, A., Philippsen, P., and Pringle, J.R. (1998). Additional modules for versatile and economical PCR-based gene deletion and modification in Saccharomyces cerevisiae. Yeast *14*, 953–961.

Lorsch, J.R., and Herschlag, D. (1998). The DEAD box protein eIF4A. 1. A minimal kinetic and thermodynamic framework reveals coupled binding of RNA and nucleotide. Biochemistry *37*, 2180–2193.

McConnell, T.S., Cech, T.R., and Herschlag, D. (1993). Guanosine binding to the Tetrahymena ribozyme: thermodynamic coupling with oligonucleotide binding. Proc. Natl. Acad. Sci. USA *90*, 8362–8366.

Miller, O.L., Jr., and Beatty, B.R. (1969). Visualization of nucleolar genes. Science *164*, 955–957.

Mohr, D., Wintermeyer, W., and Rodnina, M.V. (2002). GTPase activation of elongation factors Tu and G on the ribosome. Biochemistry *41*, 12520–12528.

Muhlberg, A.B., Warnock, D.E., and Schmid, S.L. (1997). Domain structure and intramolecular regulation of dynamin GTPase. EMBO J. *16*, 6676–6683.

Narayanan, R., Leonard, M., Song, B.D., Schmid, S.L., and Ramaswami, M. (2005). An internal GAP domain negatively regulates presynaptic dynamin in vivo: a two-step model for dynamin function. J. Cell Biol. *169*, 117–126.

Osheim, Y.N., French, S.L., Keck, K.M., Champion, E.A., Spasov, K., Dragon, F., Baserga, S.J., and Beyer, A.L. (2004). Pre-18S ribosomal RNA is structurally compacted into the SSU processome prior to being cleaved from nascent transcripts in Saccharomyces cerevisiae. Mol. Cell *16*, 943–954.

Palm, G.J., Billy, E., Filipowicz, W., and Wlodawer, A. (2000). Crystal structure of RNA 3′-terminal phosphate cyclase, a ubiquitous enzyme with unusual topology. Struct. Fold. Des. *8*, 13–23.

Peluso, P., Herschlag, D., Nock, S., Freymann, D.M., Johnson, A.E., and Walter, P. (2000). Role of 4.5S RNA in assembly of the bacterial signal recognition particle with its receptor. Science *288*, 1640–1643.

Peluso, P., Shan, S.O., Nock, S., Herschlag, D., and Walter, P. (2001). Role of SRP RNA in the GTPase cycles of Ffh and FtsY. Biochemistry *40*, 15224–15233.

Pingoud, A., Block, W., Wittinghofer, A., Wolf, H., and Fischer, E. (1982). The elongation factor Tu binds aminoacyl-tRNA in the presence of GDP. J. Biol. Chem. *257*, 11261–11267.

Pingoud, A., and Urbanke, C. (1980). Aminoacyl transfer ribonucleic acid binding site of the bacterial elongation factor Tu. Biochemistry *19*, 2108–2112.

Rodnina, M.V., Savelsbergh, A., Katunin, V.I., and Wintermeyer, W. (1997). Hydrolysis of GTP by elongation factor G drives tRNA movement on the ribosome. Nature *385*, 37–41.

Rodnina, M.V., and Wintermeyer, W. (2001). Fidelity of aminoacyl-tRNA selection on the ribosome: kinetic and structural mechanisms. Annu. Rev. Biochem. *70*, 415–435.

Romero, G., Chau, V., and Biltonen, R.L. (1985). Kinetics and thermodynamics of the interaction of elongation factor Tu with elongation factor Ts, guanine nucleotides, and aminoacyl-tRNA. J. Biol. Chem. *260*, 6167–6174.

Sanchez, R., and Sali, A. (1998). Large-scale protein structure modeling of the Saccharomyces cerevisiae genome. Proc. Natl. Acad. Sci. USA *95*, 13597–13602.

Shan, S.O., and Herschlag, D. (1996). Energetic effects of mulitple hydrogen bonds. Implications for enzymatic catalysis. J. Amer. Chem. Soc. *118*, 5515–5518.

Song, B.D., and Schmid, S.L. (2003). A molecular motor or a regulator? Dynamin's in a class of its own. Biochemistry *42*, 1369–1376.

Steiner-Mosonyi, M., Leslie, D.M., Dehghani, H., Aitchison, J.D., and Mangroo, D. (2003). Utp8p is an essential intranuclear component of the nuclear tRNA export machinery of Saccharomyces cerevisiae. J. Biol. Chem. *278*, 32236–32245.

Tuma, P.L., Stachniak, M.C., and Collins, C.A. (1993). Activation of dynamin GTPase by acidic phospholipids and endogenous rat brain vesicles. J. Biol. Chem. *268*, 17240–17246.

van Hoof, A., Lennertz, P., and Parker, R. (2000). Three conserved members of the RNase D family have unique and overlapping functions in the processing of 5S, 5.8S, U4, U5, RNase MRP and RNase P RNAs in yeast. EMBO J. *19*, 1357–1365.

Venema, J., and Tollervey, D. (1996). RRP5 is required for formation of both 18S and 5.85 rRNA in yeast. EMBO J. *15*, 5701–5714.

Venema, J., and Tollervey, D. (1999). Ribosome synthesis in Saccharomyces cerevisiae. Annu. Rev. Genet. *33*, 261–311.

Warnock, D.E., Hinshaw, J.E., and Schmid, S.L. (1996). Dynamin self-assembly stimulates its GTPase activity. J. Biol. Chem. *271*, 22310–22314.

Wegierski, T., Billy, E., Nasr, F., and Filipowicz, W. (2001). Bms1p, a G-domain-containing protein, associates with Rcl1p and is required for 18S rRNA biogenesis in yeast. RNA *7*, 1254–1267.

Wehner, K.A., and Baserga, S.J. (2002). The sigma(70)-like motif: a eukaryotic RNA binding domain unique to a superfamily of proteins required for ribosome biogenesis. Mol. Cell *9*, 329–339.

Winzeler, E.A., Shoemaker, D.D., Astromoff, A., Liang, H., Anderson, K., Andre, B., Bangham, R., Benito, R., Boeke, J.D., Bussey, H., et al. (1999). Functional characterization of the S. cerevisiae genome by gene deletion and parallel analysis. Science *285*, 901–906.